

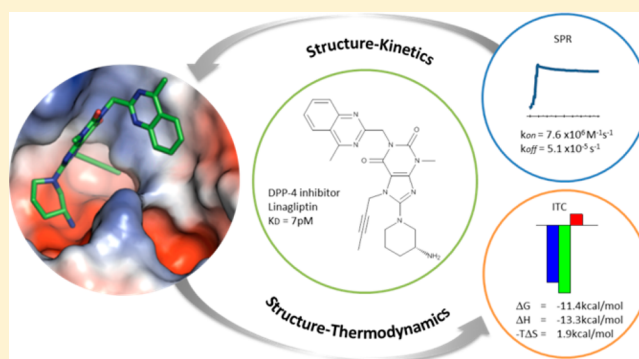
Comparative Analysis of Binding Kinetics and Thermodynamics of Dipeptidyl Peptidase-4 Inhibitors and Their Relationship to Structure

Gisela Schnapp,[†] Thomas Klein,[‡] Yvette Hoevels,[†] Remko A. Bakker,[‡] and Herbert Nar^{*,†}

[†]Department of Lead Identification and Optimization Support and [‡]Department of CardioMetabolic Diseases Research, Boehringer Ingelheim Pharma GmbH & Co. KG, Biberach 88397, Germany

S Supporting Information

ABSTRACT: The binding kinetics and thermodynamics of dipeptidyl peptidase (DPP)-4 inhibitors (gliptins) were investigated using surface plasmon resonance and isothermal titration calorimetry. Binding of gliptins to DPP-4 is a rapid electrostatically driven process. Off-rates were generally slow partly because of reversible covalent bond formation by some gliptins, and partly because of strong and extensive interactions. Binding of all gliptins is enthalpy-dominated due to strong ionic interactions and strong solvent-shielded hydrogen bonds. Using a congeneric series of molecules which represented the intermediates in the lead optimization program of linagliptin, the onset of slow binding kinetics and development of the thermodynamic repertoire were analyzed in the context of incremental changes of the chemical structures. All compounds rapidly associated, and therefore the optimization of affinity and residence time is highly correlated. The major contributor to the increasing free energy of binding was a strong increase of binding enthalpy, whereas entropic contributions remained low and constant despite significant addition of lipophilicity.



INTRODUCTION

Dipeptidyl peptidase (DPP)-4 is a widely distributed, membrane-bound, but also secreted, serine protease. It is responsible for the rapid inactivation of the incretin hormones glucagon-like peptide (GLP)-1 and glucose-dependent insulinotropic peptide (GIP) via cleavage of a dipeptide from the N-terminus of these oligopeptides.¹ GLP-1 and GIP are released from the gut in response to food intake and exert a potent glucose-dependent insulinotropic action, thereby contributing to the maintenance of postprandial glycemic control.² GLP-1 is also involved in the inhibition of postprandial glucagon secretion from pancreatic α -cells, retardation of gastric emptying, suppression of appetite leading to reduction in food intake, and direct beneficial effects on pancreatic β -cells.^{3,4} Inhibition of DPP-4 prolongs the residence time and consequently the activity of GLP-1 and GIP. Inhibition of GLP-1 and GIP metabolic breakdown improves glycemic control in patients with type 2 diabetes, making DPP-4 a good therapeutic target.⁵

Dipeptidyl Peptidase-4. DPP-4 is a serine exodipeptidase and a member of the prolyl oligopeptidase family. It is highly specific in recognizing peptide substrates with proline or alanine in the last position (P1) prior to the scissile amide bond. DPP-4 exists as a homodimer consisting of 766 amino acids with cytoplasmic, transmembrane, and extracellular regions. The extracellular part is divided into a β -propeller domain and a catalytic $\alpha\beta$ -hydrolase domain with the catalytic

triad Ser630–Asp708–His740.⁶ The active site of the DPP-4 enzyme lies within a large cavity formed by these domains and includes the catalytic Ser630 and the oxyanion hole (Tyr631, Tyr547), a hydrophobic S1 pocket (Tyr631, Val656, Trp659, Tyr662, Tyr666, and Val711), and an S2 pocket. Substrates can access the active site through a tunnel in the β -propeller or via a side opening.

Approved DPP-4 Inhibitors. Several DPP-4 inhibitors (gliptins) have been successfully launched and have shown clinically good efficacy and safety in patients with type 2 diabetes. The currently worldwide marketed DPP-4 inhibitors sitagliptin, vildagliptin, saxagliptin, linagliptin, alogliptin, and teneligliptin (tenegliptin launched in Japan and Argentina) have distinct chemical structures that confer different potency and selectivity profiles, as well as pharmacokinetic and pharmacologic properties, and display different modes of binding.^{7–9} Vildagliptin and saxagliptin are peptide mimetic compounds, which were discovered by building on the substrate-derived Gly–Pro dipeptide scaffold. Teneligliptin was developed from a prolylthiazolidine core as a proline mimetic.¹⁰ In contrast, sitagliptin, alogliptin, and linagliptin were developed through screening and lead optimization (LO).

Structural Information on Gliptin Binding to DPP-4. X-ray cocrystal structures of all gliptins are reported (see Yoshida

Received: March 31, 2016

Published: July 20, 2016



et al.,¹⁰ Eckhardt et al.,¹¹ and Nabeno et al.⁹ and references therein). Although the chemical structures are different, all DPP-4 inhibitors are substrate-competitive active site binders and have common interactions with key residues of the target protein. Primary or secondary amino groups interact with the recognition site for the peptide substrate N-terminus (Glu205, Glu206, and Tyr662, the “amino hot spot”) of DPP-4 via the formation of two or three charge-reinforced hydrogen bonds. The hydrophobic S1 pocket of DPP-4 is occupied by hydrophobic inhibitor moieties, while the S2 pocket is filled by other substituents.

Vildagliptin and saxagliptin are cyanopyrrolidine inhibitors and form a covalent but reversible complex with DPP-4 through the formation of an imino ester with the hydroxyl group of the catalytic serine S630. Both inhibitors have a bulky adamantyl group that occupies the S2 pocket in a similar position but with the hydroxyl group in different orientations (Figure 1a). Both vildagliptin and saxagliptin bind to the target without inducing any conformational change to the protein. Tenoeligliptin and sitagliptin occupy the active site in a linear conformation (Figure 1b). Their binding leads to a conformational change involving Arg358, which adopts a distinct side chain orientation that facilitates the opening of a hydrophobic pocket termed the extended S2 pocket. The phenyl and trifluoromethyl moieties of sitagliptin and teneligliptin, respectively, occupy this induced pocket. The binding of linagliptin and alogliptin to DPP-4 is accompanied by a different conformational change involving Tyr547, which allows the formation of a π -stacking interaction with the xanthine and uracil cores of linagliptin and alogliptin, respectively. Both inhibitors form an H-bond with the backbone NH of Tyr631 utilizing a carbonyl oxygen H-bond acceptor group in their heterocyclic cores. The binding of linagliptin to DPP-4 involves extensive hydrophobic interactions of its 1-quinazoline substituent within the S1'–S2' pockets, mainly with the Trp629 indole side chain (Figure 1c). It should be noted that the crystal structures that will be used below to discuss structure–biophysics relationships were derived from two orthologs of DPP-4 (porcine for linagliptin precursors 1 and 2 and human for all others), from distinct crystal forms, and cocrystals were obtained under different conditions. However, as discussed above, the ligand binding site of DPP-4 is in a large cavity, and therefore, distinct crystal packing will probably not affect the ligand binding mode and interaction patterns.

Binding Kinetics and Thermodynamics in Drug Discovery. During the drug discovery process, there is considerable interest in the key parameters of binding kinetics and thermodynamics for compound selection and optimization.^{12–16} For instance, drugs with prolonged off-rates may be attractive from a pharmacologic perspective because once bound to the target, they can potentially inhibit the enzyme function even after the free drug has been cleared from circulation. This rare situation occurs if the binding kinetics of the drug are much slower than its pharmacokinetics.

It is discussed widely in the literature that selection of compounds with a strong contribution of enthalpy to the free energy of binding is advised in the early phases of a drug discovery process because chemical optimization often involves the addition of hydrophobic groups which mainly impact binding entropy. Binding enthalpy, in contrast, is more difficult to optimize.^{15,17} Although increasing numbers of publications describe experimental data, the molecular determinants of binding kinetic and thermodynamic profiles are still only

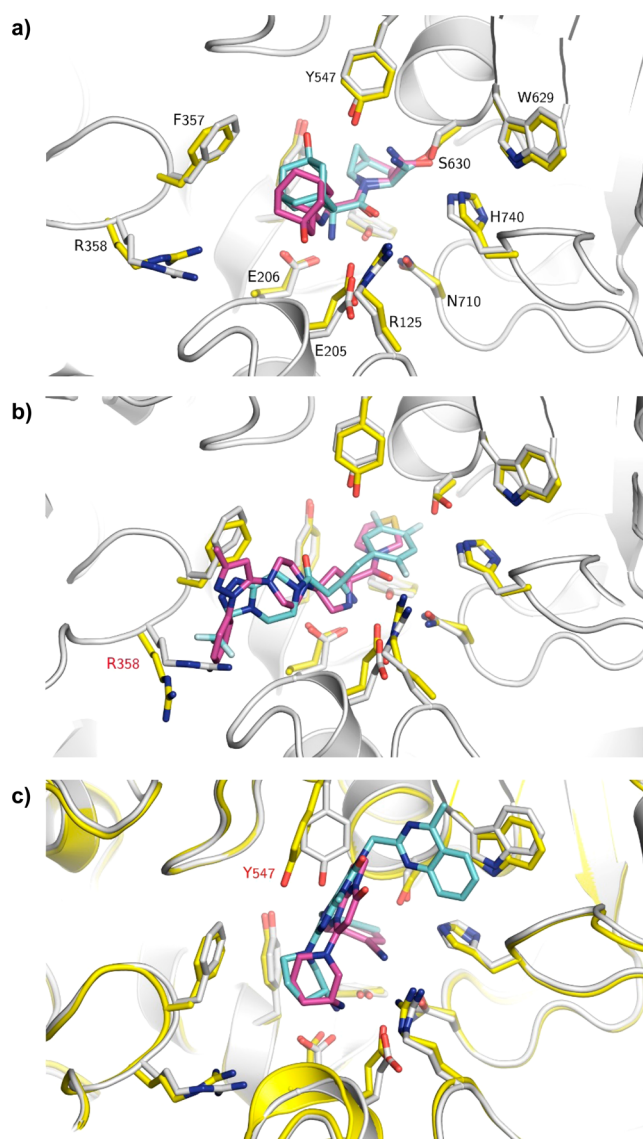


Figure 1. Co-structures of DPP-4 inhibitors bound within the DPP-4 active site. DPP-4 inhibitors with a similar binding mode in X-ray structures are shown as overlaid pairs: (a) DPP-4 active site with saxagliptin (3BJM,²³ cyan) and vildagliptin (3W2T,⁹ purple) bound; (b) DPP-4 active site with sitagliptin (1X70,⁴⁸ cyan) and teneligliptin (3VJK,¹⁰ purple) bound; (c) DPP-4 active site with linagliptin (2RGU,¹¹ cyan) and alogliptin (3G0B,⁴⁹ purple) bound. In each panel, a superposition of the structures of free (white carbon atoms) and ligand bound (yellow carbon atoms) enzyme shows protein structural changes upon ligand binding. Key interaction residues are indicated in black; residues involved in structural rearrangements upon binding are indicated in red. Protein data bank (PDB) accession codes for the various X-ray structures are indicated in parentheses above.

scarcely understood, and comprehensive information on the development of these parameters in a congeneric series of compounds remains rare.

DPP-4 inhibitors are known to have relatively long residence times on their target protein.^{7,18,19} However, no comparative studies of biophysically derived binding kinetics for the approved DPP-4 inhibitors have been reported to date. In the present study, we investigated the binding kinetics and thermodynamics of DPP-4 inhibitors using surface plasmon resonance (SPR) and isothermal titration calorimetry (ITC) studies. In addition, a retrospective biophysical study was

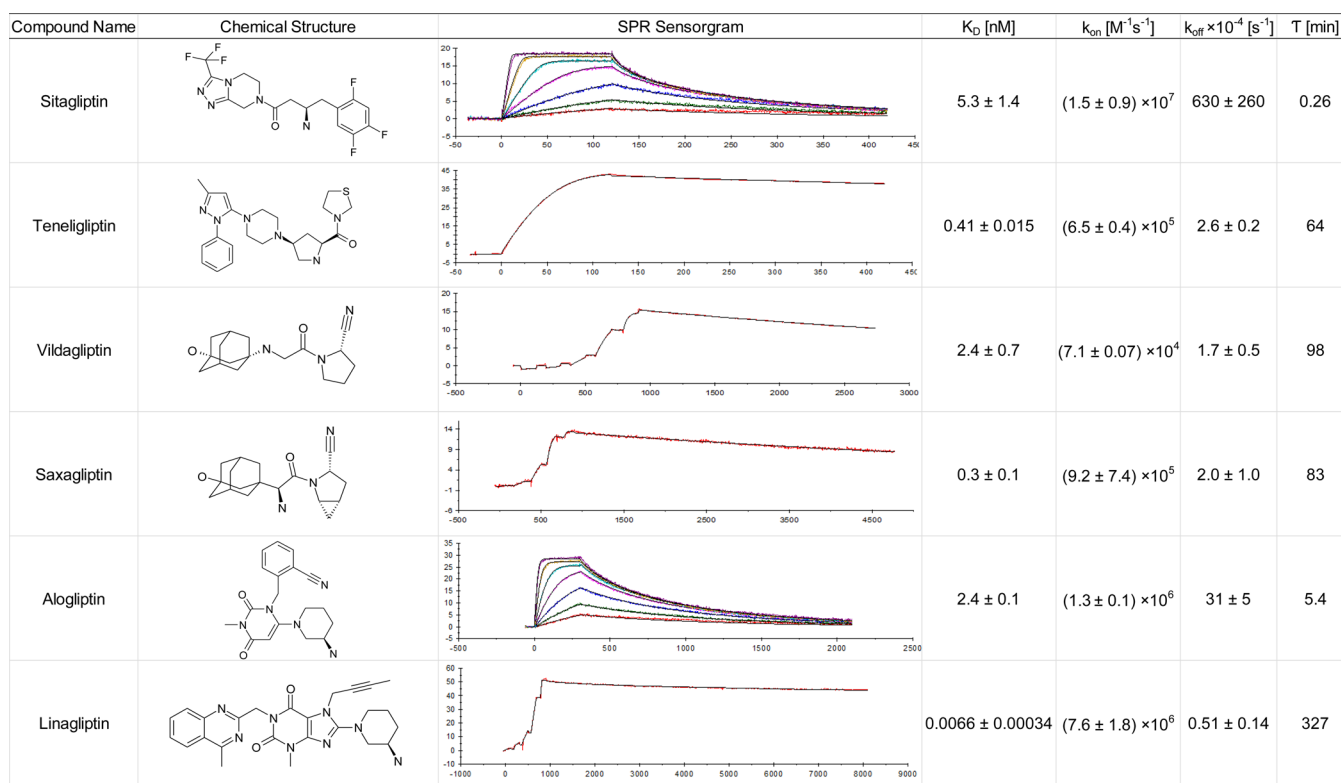


Figure 2. Binding kinetics of approved DPP-4 inhibitors studied with surface plasmon resonance. Sitagliptin and alogliptin were studied using multicycle binding kinetics, whereas the other DPP-4 inhibitors were studied using single-cycle kinetics. Teneligliptin is shown and fitted as a single concentration measurement. The x -axis in the sensorgrams represents the time in seconds; the y -axis represents the signal in responsive units. The colored lines represent experimental data, and the black line represents the fitted curve. The sensorgrams show representative examples. The kinetic data were mean values from two independent measurements with calculated standard deviation. Residence time τ was calculated as the reciprocal of the mean k_{off} value ($\tau = 1/k_{off}$).

conducted on a series of congeneric compounds representing intermediates in the drug discovery process leading to linagliptin. Results will be discussed regarding the binding modes of these compounds to the DPP-4 active site, and some conclusions will be made concerning emerging structure–kinetic and structure–thermodynamic relationships.

RESULTS AND DISCUSSION

Gliptins Are Low Nanomolar or Subnanomolar Inhibitors of Human DPP-4. Linagliptin was the most potent inhibitor of DPP-4 activity using human recombinant enzyme or enzyme derived from human plasma. The IC_{50} was 1.4 nM (Supporting Information Table S1), which is consistent with data previously published by Thomas et al. using human Caco-2 cell extracts.²⁰ With an enzyme concentration of approximately 1 nM in both assays, the activity of linagliptin is most probably beyond the detection limit (assay wall) so that its IC_{50} reflects an upper limit to its real potency.

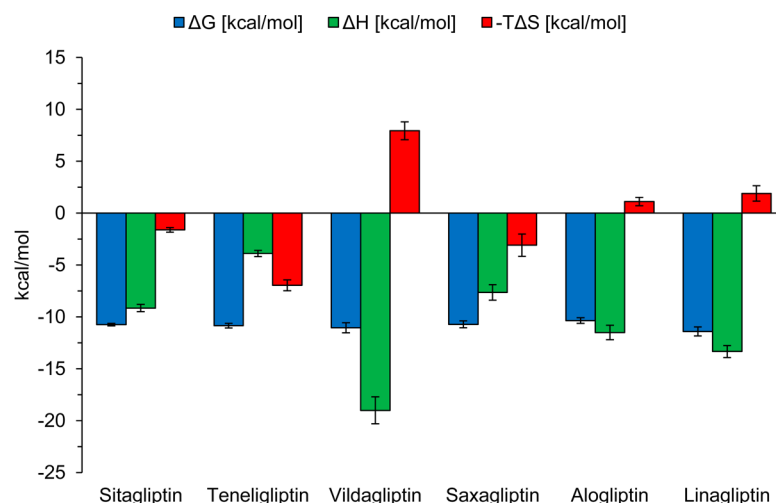
The other DPP-4 inhibitors showed lower potencies, ranging from 7 nM for alogliptin to 95 nM for vildagliptin (Supporting Information Table S1). Teneligliptin was the only DPP-4 inhibitor that showed a weaker affinity for the enzyme derived from human plasma than for the human recombinant enzyme. However, the numerical differences were relatively small and may lie within the analytical variability of the assay.

DPP-4 Inhibitors Associate Rapidly with Their Target. SPR sensorgrams describing the binding kinetics of each DPP-4 inhibitor are shown in Figure 2. Quantitative data analysis indicated that linagliptin is a low picomolar binder with the

highest affinity for DPP-4, followed by saxagliptin and teneligliptin which exhibited binding affinities of 0.3 nM and 0.4 nM, respectively. Sitagliptin, alogliptin, and vildagliptin were significantly less potent with low single-digit nanomolar binding affinities.

The on-rates of all DPP-4 inhibitors were generally fast and within the range of 10^5 – 10^7 $M^{-1}s^{-1}$. On-rates of the primary amines (alogliptin, sitagliptin, saxagliptin, and linagliptin) were close to the diffusion limit ($>10^6$ $M^{-1}s^{-1}$), whereas the secondary amines (vildagliptin and teneligliptin) and saxagliptin were associated with at least 10-fold slower on-rates (approximately 10^5 $M^{-1}s^{-1}$). For example, for the two structurally similar reversible covalent inhibitors vildagliptin and saxagliptin, the on-rate of the secondary amine vildagliptin was 7.1×10^4 $M^{-1}s^{-1}$, whereas the primary amine saxagliptin showed a faster on-rate of 9.2×10^5 $M^{-1}s^{-1}$.

There is ample evidence in the current literature, summarized in a review by Pan et al.,²¹ which shows that electrostatic interactions between a charged drug and a reversely charged protein positively impact association rates. On the basis of this evidence, we assumed that binding of gliptins to DPP-4 is a rapid electrostatically driven process with an influence of attractive Coulomb forces on the association rates. The localized positive charge on the ligand is sensed by the negatively charged surface patch at the Glu205/6 dyad in the DPP-4 active site leading to an acceleration of the bimolecular binding process. Because the charge density on the ammonium functions is higher for primary than secondary amines, the former amines exhibit a faster association rate than the latter.



Compound	ΔG [kcal/mol]	ΔH [kcal/mol]	$-T\Delta S$ [kcal/mol]	K_D [nM]
Sitagliptin	-10.74 ± 0.12	-9.14 ± 0.35	-1.61 ± 0.23	13.5 ± 2.7
Teneligliptin	-10.84 ± 0.22	-3.89 ± 0.31	-6.95 ± 0.52	11.9 ± 4.2
Vildagliptin	-11.05 ± 0.48	-19.00 ± 1.30	7.94 ± 0.85	10.7 ± 7.2
Saxagliptin	-10.72 ± 0.33	-7.64 ± 0.75	-3.09 ± 1.08	15.9 ± 7.9
Alogliptin	-10.35 ± 0.27	-11.50 ± 0.70	1.11 ± 0.41	28.5 ± 12.3
Linagliptin	-11.40 ± 0.44	-13.33 ± 0.57	1.90 ± 0.75	5.3 ± 3.6

Figure 3. Thermodynamic profiles of the gliptins binding to DPP-4 based on isothermal titration calorimetry experiments. Experimentally derived parameters include the Gibbs free energy of binding (ΔG , blue bar), the enthalpy change (ΔH , green bar), and the temperature-dependent entropy change ($-T\Delta S$, red bar). 40 μ M DPP-4 was titrated into 5 μ M DPP-4 inhibitor. Data are mean values from at least two titrations with calculated standard deviation.

Structurally Distinct DPP-4 Inhibitors Exhibit Distinct Target Dissociation Behavior. Sitagliptin and alogliptin had relatively fast off-rates of 0.063 s^{-1} and 0.0031 s^{-1} , respectively. The covalent binders vildagliptin and saxagliptin had much slower dissociation rates of $1.7 \times 10^{-4} \text{ s}^{-1}$ and $2.0 \times 10^{-4} \text{ s}^{-1}$, respectively. The off-rate of teneligliptin was slow ($2.6 \times 10^{-4} \text{ s}^{-1}$) and similar to the covalent binders. Linagliptin had the slowest dissociation rate ($5.1 \times 10^{-5} \text{ s}^{-1}$), corresponding to a residence time of 327 min (Figure 2).

For the slowly dissociating compounds, SPR experiments had to be performed in a single-cycle kinetics setting, and dissociation times needed to be sufficiently long to observe a significant decline in the sensorgrams. This was especially the case for linagliptin, where values were at the detection limit of the instrumentation. Validation of the SPR-derived dissociation rates was therefore sought through comparisons with other kinetic data for gliptins from the literature. There are two reports on DPP-4 inhibitor binding kinetics based on enzyme kinetics for four of the six compounds under investigation. The k_{off} values determined using SPR are in good agreement with off-rates obtained by enzyme activity recovery assays reported by Thomas et al. (linagliptin $3.0 \times 10^{-5} \text{ s}^{-1}$; vildagliptin $2.1 \times 10^{-4} \text{ s}^{-1}$)²⁰ and Wang et al. (saxagliptin $2.3 \times 10^{-4} \text{ s}^{-1}$; sitagliptin $>5.8 \times 10^{-3} \text{ s}^{-1}$).²²

Structure–Kinetic Relationships. The dissociation rates of the gliptins range from a relatively fast off-rate regime (sitagliptin and alogliptin with residence times of 0.26 and 5.4 min, respectively) to a slow off-rate regime (327 min for linagliptin). This slow dissociation behavior can be attributed

either to reversible covalent bond formation (saxagliptin and vildagliptin) or to strong and extensive interactions that both pose a large energy barrier for dissociation (teneligliptin and linagliptin).

The reversible covalent binders vildagliptin and saxagliptin show very similar interactions in their active sites and do not induce any conformational change in the protein. Both inhibitors have nanomolar affinities and prolonged off-rates resulting in residence times of the corresponding enzyme complexes of approximately 1.5 h. We assumed that the slow dissociation kinetics is a result of the increased activation barrier posed by the cleavage of the imino ester bonds involving S630. Although the associated reaction kinetics for the ester bond cleavage is fast, it is the stability of the covalent complexes that leads to a substantial contribution to off-rate prolongation. For saxagliptin a close analog lacking the cyano warhead exhibits a 20-fold lower K_i .²³ Assuming similar on-rates for the pair of compounds, the analog should dissociate 20-fold faster than saxagliptin, yielding a compound with fast binding kinetics.

The essential structural elements for the long residence times of teneligliptin and linagliptin presumably are moieties that either form enhanced hydrogen-bonding interactions or cover larger hydrophobic surface areas. This assumption is supported by literature reports suggesting a prominent role of hydrogen bonds that are shielded from water by surrounding hydrophobic regions in the optimization of residence times.²⁴ For example, from a comparison of linagliptin and alogliptin, the 1-quinazoline group of linagliptin covers a large hydrophobic surface patch in the S1'–S2' region of the DPP-4 active site,

mainly with the Trp629 indole side chain, and simultaneously shields the hydrogen bond of its core carbonyl oxygen to the backbone NH of Tyr631. The analogous hydrogen bond of alogliptin is hydrophobically shielded to a lesser extent because of the absence of a hydrophobic substituent in an analogous position. As a result, the hydrogen bond is more exposed to solvent and more easily replaced by water. Therefore, significantly higher binding affinity and slower dissociation of linagliptin compared with alogliptin may in part be explained by an efficient solvent-shielding effect of this crucial hydrogen bond.

Conformational changes are a prominent feature of many protein–ligand interactions with slow dissociation kinetics.^{12,25} Binding of some gliptins is associated with a change in the conformation of the DPP-4 active site, mainly because of side chain rotations about Arg358 (sitagliptin and teneligliptin) or Tyr547 (linagliptin and alogliptin).

Surprisingly, in the present study, pairs of DPP-4 inhibitors that have similar binding to the active site of DPP-4 show dissimilar binding kinetics (Supporting Information Figure S1). Teneligliptin and sitagliptin induce the same conformational change involving Arg358 and in a similar way occupy the induced hydrophobic extended S2 pocket with their phenyl and trifluoromethyl moieties. However, these common hydrophobic interactions in the extended S2 pocket as well as the necessary conformational changes seem to have no dominant role in binding kinetics because sitagliptin has a much faster off-rate than teneligliptin.

The binding of linagliptin and alogliptin to DPP-4 is accompanied by a different conformational change involving Tyr547, which allows the formation of a π -stacking interaction with the xanthine core of linagliptin. Again, this conformational change has no dominant role in determining binding kinetics because both inhibitors differ in their off-rates by 2 orders of magnitude.

Gliptins Are Enthalpic DPP-4 Binders. ITC measures the binding enthalpy by detecting the heat absorbed or released during a bimolecular binding event. One limitation of ITC is its application to compounds with extraordinarily high potency, such as some of the DPP-4 inhibitors used in this study. The calculation of the association constant K_a from the slope of the binding isotherm in such a case is problematic owing to its steepness. The most potent DPP-4 inhibitor, linagliptin, showed the steepest binding isotherm, requiring therefore that the K_D value for linagliptin be determined using a complementary competition experiment. Use of the competitor led to the expected significantly lower K_D value and to minor changes in the thermodynamic signature of linagliptin (Supporting Information Figure S2). For the other DPP-4 inhibitors, the binding isotherms were well fitted (Supporting Information Figure S3). Therefore, determination of the entropic and enthalpic contributions was possible and comparisons were made using the derived data. For consistency, the thermodynamic signature of linagliptin from direct ITC in the absence of a competitor ligand was used to compare it with the other gliptins. Binding of all DPP-4 inhibitors was driven by strong enthalpic contributions. Relatively minor entropic contributions were observed (Figure 3).

The partially solvent-shielded charge-reinforced hydrogen bonds formed between the cationic primary and secondary amines of the inhibitors and the active site amino hot-spot pharmacophore, representing the major interaction formed by

all DPP-4 inhibitors, may be the major component of the strong enthalpic contribution.

Alogliptin and linagliptin have comparable thermodynamic signatures that correspond to their similar binding interactions. However, despite a similar binding mode and inhibition mechanism, vildagliptin and saxagliptin displayed significantly different binding thermodynamics. Binding of vildagliptin exhibited a substantial entropic penalty, which was compensated for by a much larger enthalpic contribution to binding, resulting in similar free energies of binding for the two covalent inhibitors. This finding is difficult to interpret using existing structural information. A plausible explanation for this phenomenon may be that the orientation of the hydroxyadamantyl group is inverted between the two complex structures, despite identical substructures and similar intermolecular interactions. The different ligand orientations will have a significant effect on the surrounding water structure which was shown previously to have a major impact on the partitioning of free energy.^{17,26,27}

Both teneligliptin and sitagliptin had favorable entropic contributions to the binding energy that could result from desolvation because of hydrophobic interactions in the extended S2 pocket. In contrast to sitagliptin, teneligliptin has a secondary amine that can form only two hydrogen bonds with the amino hot spot. This may be the reason for diminished binding enthalpy.

In recent years, detailed analyses of binding thermodynamics for a number of model systems have been published, including the interpretation of the dominating role of the water structure using high resolution crystallographic structural information (<1.5 Å).¹⁷ Protein–ligand costructures with very high resolution and quality are required to allow complete modeling of the solvent structure around the binding site and its comparison with the solvent structure in the nonliganded protein. For the gliptins, structures were determined at 2.1–2.6 Å resolution. Inspection of the structural models and the corresponding electron densities showed that despite almost equivalent reported resolution, the quality of the experimental data, manifested in the electron densities, and the extent to which the data were used to model the water structure deviate significantly. Consequently, a comparative interpretation of the role of the water structure for the gliptins is precluded. For instance, although the two covalently bound gliptins saxagliptin (3BJM) and vildagliptin (3W2T) were determined at practically identical resolutions (2.35 Å), the elaboration of the solvent structure is dramatically different (with 2/3 versus 13/13 modeled water molecules in the two protomers in the asymmetric unit). For saxagliptin, more water molecules could actually be built into the model based on an analysis of the difference electron density. Future work on this aspect could utilize *in silico* approaches such as WaterMap^{28,29} or GIST^{30,31} to obtain estimates of solvent energies using explicit solvent modeling in addition to the crystallographic information.

Comparison of Quantitative Binding and Potency Data, and Validity of Biophysical Data. In the above, quantitative binding and activity data for the family of DPP-4 inhibitors have been presented. A direct comparison of the data showed that the calculated binding affinities (K_D) from SPR data are numerically lower than those determined using a biochemical assay or ITC. A plausible explanation for this difference is that for the enzymatic activity data, a lower limit to the IC_{50} is set by the assay wall which is in the 1 nM range in

the current experimental setting, whereas the higher sensitivity SPR method is not limited by any assay wall.

In ITC, as described above, the high potency of the compounds and the corresponding steepness of the binding isotherms may result in a systematic overestimation of the K_D . In such a scenario, application of competition ITC is indicated to derive more reliable K_D values. However, the addition of a competing ligand may also affect the thermodynamic signature.³²

The K_D calculations from SPR experiments could be influenced by a mass transport limitation.³³ Moreover, the curve fitting in SPR for very slow off-rates (e.g., for linagliptin) is at the limit of the instrument's specification. The long wash-out times required for a significant level of dissociation may be confounded by target dissociation from the sensor surface and therefore could cause uncertainty in the calculation of the K_D value. However, the off-rates obtained by SPR are in good agreement with values obtained by enzymatic activity recovery assays.

In all assays, linagliptin consistently had, by far, the highest affinity and the longest residence time among DPP-4 inhibitors.

Biophysical Analysis of a Congeneric Series of Linagliptin Precursors. In the early phases of an LO program in medicinal chemistry, optimization of a given lead candidate traditionally involves improving its binding affinity. In contrast, recent discussions in the field have focused on the importance of using binding kinetics, especially the dissociation rate, as the primary optimization parameter and binding thermodynamics as a key element of lead selection.^{15,34–37}

Here, the current retrospective analysis has reviewed a congeneric series of DPP-4 inhibitors. SPR and ITC were used to determine how the kinetic and thermodynamic signatures of the binding event developed during the optimization process, leading to the development of linagliptin.

Xanthine derivative **1** was discovered using a high-throughput screening (HTS) process and showed promising inhibitory activity in the low micromolar range (Figure 4a). The focus of the LO program was on the variation of

substituents at positions 1, 3, 7, and 8 of the xanthine core. In the initial phases, a 50-fold increase in potency was achieved by replacing the 8-piperazine moiety with a 3-aminopiperidine (Figure 4b). Further variations at position 1, made by attaching hydrophobic/aromatic substituents like benzyl, phenethyl, or phenacetyl, increased the potency by a factor of 15. Compound **3** (Figure 4c) was the first long-acting inhibitor in the lead series with an IC_{50} of 5 nM. However, this compound showed unacceptably high inhibition of hERG channels (IC_{50} = 200 nM) and a high affinity for muscarinic receptors M1 (50 nM), M2, and M3 (both ~150 nM). Therefore, further optimization of substituents at positions 7 and 1 focused on improving the specificity profile to avoid these off-target effects. Linagliptin finally demonstrated extraordinarily high potency against DPP-4 and a clean off-target profile.^{11,20} Only the M1 receptor was inhibited at an IC_{50} of 300 nM, which is clinically irrelevant because of the low C_{max} value of 10 nM in plasma resulting from the 5 mg dose of linagliptin used in clinical practice.

In the SPR analysis, the initial HTS hit **1** showed transient binding kinetics, with a K_D value of 806 nM determined from affinity plots (Figure 5). Substitution at position 8 increased the potency (K_D = 13.2 nM) and led to a quantifiable binding kinetic profile for compound **2** (k_{off} = 0.064 s⁻¹). Compound **3** is a high affinity inhibitor (0.42 nM) with a slow off-rate of 0.00186 s⁻¹ and a residence time of 8.9 min. Finally, a further substantial increase in affinity for linagliptin is based on the considerable increased residence time of the DPP-4 complex (327 min).

On examination of the congeneric series of ligands by ITC, binding was found to be driven mainly by enthalpy. Compound affinity optimization was accompanied by increasing binding enthalpy (Figure 6 and Supporting Information Figure S4). The entropic contributions within this lead series were negligible. The initial xanthine derivative **1** had a minor favorable entropic contribution to the binding that was lost in compounds **2** and **3**. In contrast, linagliptin had a small unfavorable contribution of binding entropy.

The series of linagliptin and its precursors bind to the active site in a conserved binding mode (Figure 7). Binding of all compounds involves a conformational change of the Tyr547 side chain. This facilitates formation of a π -stacking interaction of the phenol moiety of Tyr547 and the xanthine core of the inhibitors. Further, the xanthine core forms a hydrogen bond with the C-6 carbonyl function of the xanthine scaffold to the backbone NH of Tyr631, which is another conserved interaction within the compound series. Occupation of the S1 pocket is facilitated by different hydrophobic substituents at position 7 of the xanthine core. The cationic amino functionality interacting with the amino hot spot of the active site changes from a secondary amine in compound **1** to a tertiary amine in compounds **2**, **3**, and linagliptin. The introduction of the aminopiperidine moiety in place of the piperazine ring has a strong impact on potency, mainly because its primary amino group is sterically better positioned to interact with the amino hot spot of the target active site where it can form three instead of two hydrogen bonds, leading to tighter interactions compared with the secondary amine of the initial HTS hit **1**. Finally, a more lipophilic moiety of the xanthine core is present in compound **3** and linagliptin, which leads to burial of a larger area of hydrophobic surface on the receptor by a π -stacking interaction of the quinazoline moiety with Trp629 and to an increased shielding from water of the hydrogen bond between the xanthine and the NH group of

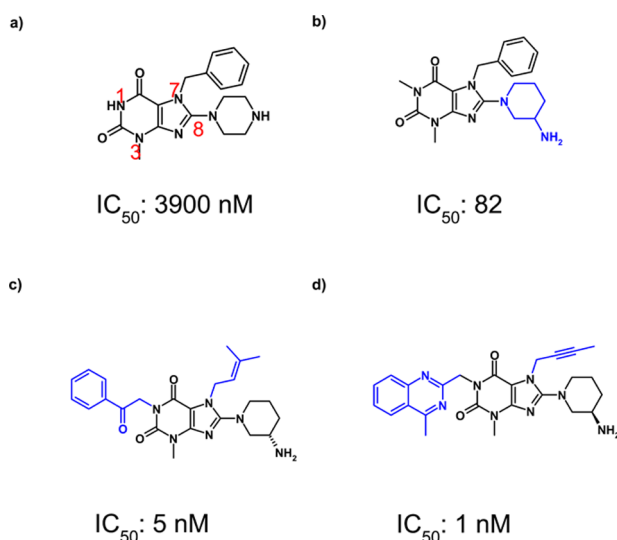


Figure 4. Chemical structures of the initial hit compound **1** from high-throughput screening (a), two precursors of linagliptin compounds **2** and **3** (b, c), and linagliptin (d). The numbers in red (a) indicate the position of the substituent in the xanthine core.

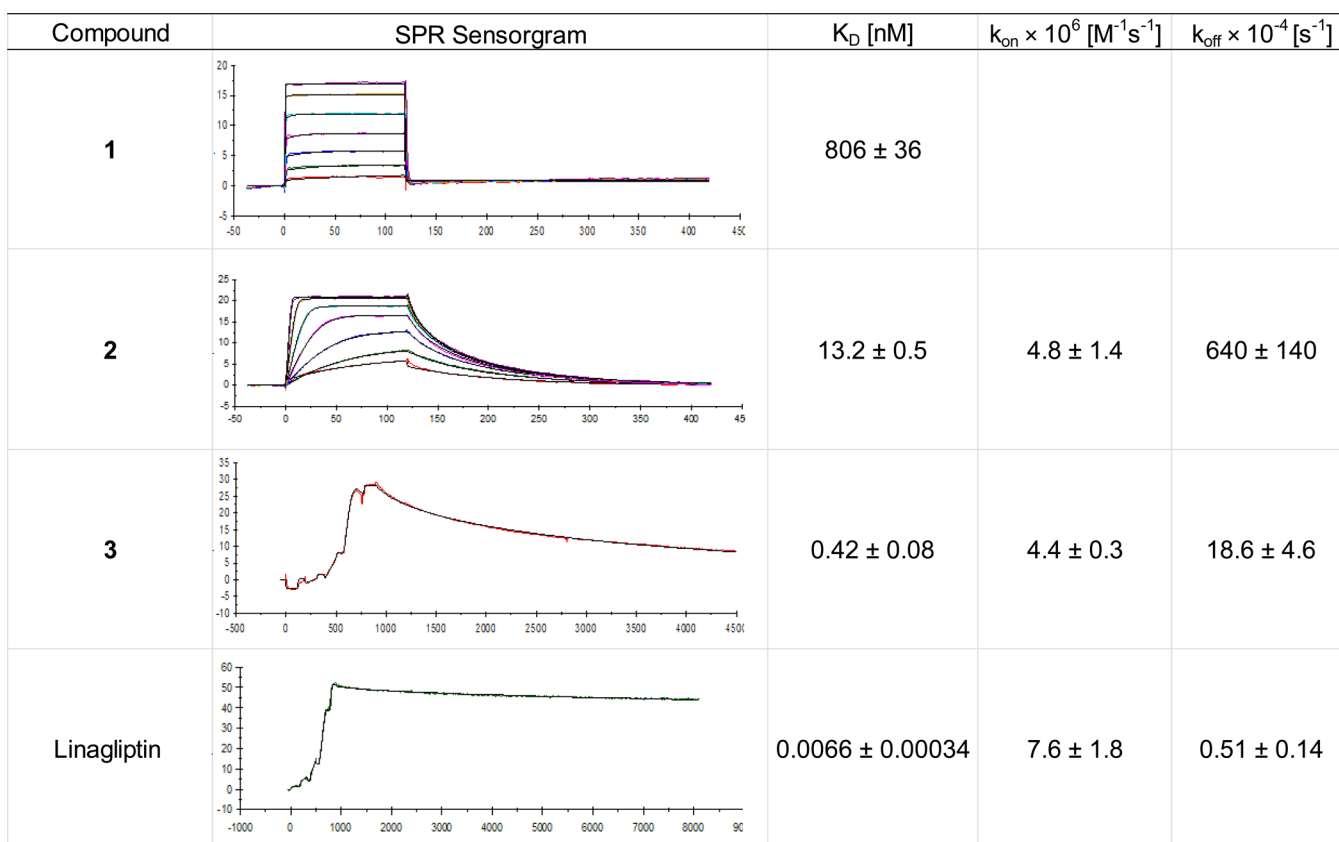


Figure 5. Binding kinetics of linagliptin precursor molecules studied with surface plasmon resonance. Compounds **1** and **2** were studied by multicycle binding kinetics, whereas compound **3** and linagliptin were studied by single-cycle kinetics. The sensorgrams show representative examples. The x -axis in the sensorgrams represents the time in seconds; the y -axis represents the signal in responsive units. The colored lines represent experimental data, and the black line represents the fitted curve. The kinetic data were mean values from two independent measurements with calculated standard deviation.

Tyr631. No considerable rearrangement of the protein structure was observed between the different ligand complexes which would produce major differences in thermodynamic signatures.

On the basis of this structural information, we conclude that the essential structural elements for off-rate improvement are the moieties that either form enhanced hydrogen bonding interactions or cover larger hydrophobic surface areas like the quinazoline group.

The on-rate in this series lies between 10^6 and $10^7 M^{-1} s^{-1}$ for all compounds and was largely unaffected during the optimization process. As mentioned above for the gliptins, it is presumed that the association process for these compounds is electrostatically dominated leading to fast on-rates close to the diffusion limit. As a consequence, during the optimization process aimed at improving affinity, the increase in residence time (decrease in k_{off}) largely develops in parallel with the binding affinity. In the case of LO of DPP-4 inhibitors, therefore, focusing on either affinity or residence time as primary optimization parameters would most probably not have affected the course of the project.

The original HTS compound **1** is a DPP-4 ligand with a dominant enthalpic contribution to the free energy of binding. The optimization process and the gain in the free energy of binding are mainly because of an increase in the enthalpic component, entropic contributions playing a minor role in the compound's thermodynamic repertoire. Only linagliptin has a small unfavorable contribution of binding entropy that may

result from entropy–enthalpy compensation for this high affinity compound.

All compounds in the congeneric series exhibit relatively low $\log D$ values (in the range of 0.0–1.6) and are thus relatively hydrophilic compounds. However, despite significant addition of lipophilicity during the optimization process (Supporting Information Figure S5), the entropic contributions were not affected; however, enthalpic contributions were increased. This trend was initially unexpected because the obvious consequence of utilizing the hydrophobic effect for improving the free energy of binding by burial of the hydrophobic surfaces and release of surface bound water molecules would be an increase in the entropic signature. Instead, the fact that the enthalpic contribution was enhanced by these additional lipophilic interactions may be interpreted by both displacement by the ligand of water molecules with high residual mobility and an improvement of the water network established on the surface of newly formed complexes. Examples of this behavior have been described previously.^{17,26,38,39}

On interpretation of these data, it should be noted that changes in the individual solvation pattern resulting from differences of just one single water molecule can strongly perturb and shift the thermodynamic signatures between ligands.^{17,26,27} In the given series of compounds, the structural information shows distinct water networks which explains why the thermodynamic profiles cannot be fully interpreted by differences in lipophilicity or interaction patterns alone.

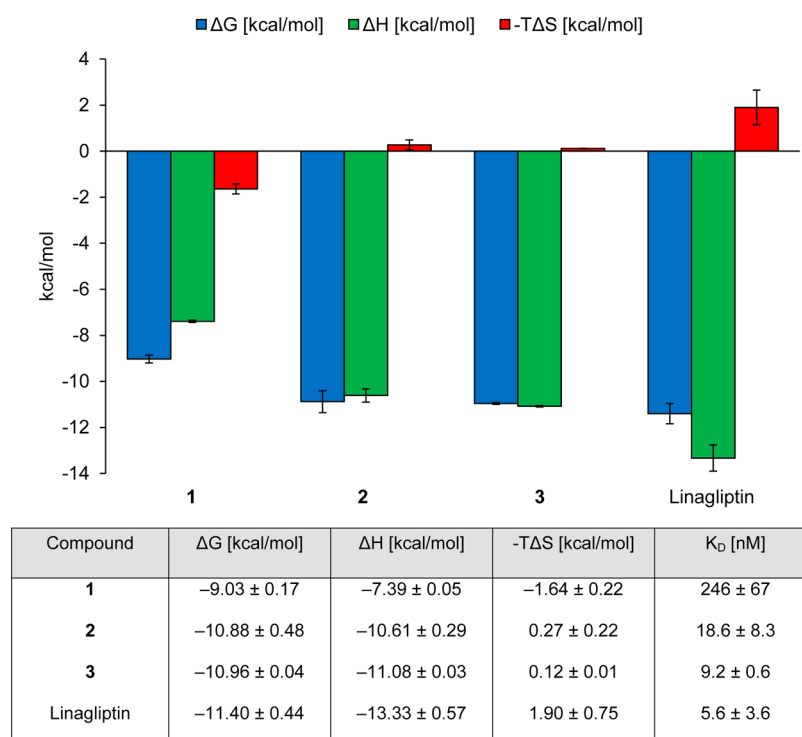


Figure 6. Thermodynamic profile of linagliptin and its precursors binding to DPP-4 based on isothermal titration calorimetry experiments. The experimentally derived parameters include the Gibbs free energy of binding (ΔG , blue bar), the enthalpy change (ΔH , green bar), and the temperature dependent entropy change ($-T\Delta S$, red bar). 40 μM 1, 2, 3, and linagliptin were titrated into 5 μM DPP-4. Data are mean values from at least two titrations with calculated standard deviation.

Finally, within the series of congeneric compounds generated in the LO program for linagliptin, a dependency was found between k_{off} values and the binding affinity/binding enthalpy. This is in line with earlier observations suggesting that longer residence times are a direct consequence of enhancing the enthalpic contributions of protein–ligand interactions.¹⁹

Relationship of Binding Kinetics and Clinical Pharmacokinetics of Linagliptin. DPP-4 inhibitors are a well established drug class for the treatment of diabetes.^{40,41} Because DPP-4 activity is inhibited by more than 80% over 24 h by most gliptins, they are administered as once-daily drugs. An exception is vildagliptin, which is administered twice daily because of its relatively short half-life.

The outstanding compound in the gliptin class is linagliptin because of its unique nonlinear pharmacokinetics and mainly nonrenal elimination ($\leq 7\%$ excreted renally).⁴² The DPP-4 protein exists in its major form as a membrane-bound protein expressed in nearly all tissues with pronounced expression in kidney and liver; it also exists in soluble form in plasma. At very low concentrations (e.g., <1 nM), 99% of linagliptin is bound to circulating DPP-4 protein in plasma and elimination is low. At higher concentrations (e.g., >100 nM), the DPP-4 protein is saturated and the proportion of protein binding decreases to 70–80%.⁴³ This results in an increase in the free fraction of linagliptin and also its volume of distribution and clearance. From those experiments, the dissociation constant of radio-labeled linagliptin to DPP-4 was determined to be in the high affinity range of 10^{-10} M,⁴³ consistent with the biochemical activity and biophysical data described above. Moreover, several studies have shown that the concentration-dependent binding and biphasic pharmacokinetic behavior of linagliptin are totally abolished in DPP-4-deficient rats or DPP-4 knockout mice,^{43,44}

indicating that a mechanism of target-mediated drug deposition dominates the pharmacokinetics of linagliptin.

An additional consequence of this unique property of linagliptin may be more relevant from a patient's perspective. With high levels of protein binding at clinically relevant linagliptin concentrations, a low level of unbound drug is available for renal filtration. For linagliptin, the renal excretion at its therapeutic dose is $<7\%$. In contrast, other DPP-4 inhibitors are eliminated primarily via the kidney. Evidence from DPP-4 knockout animals demonstrates this hypothesis, as renal clearance of linagliptin (0.01 mg/kg, iv dosing) increases from 2.7% in wild-type mice to 24.2% in the respective knockout mice.⁴³ As patients with type 2 diabetes often have impaired renal function, dose adjustment of renally cleared drugs is indicated because of the potential for drug accumulation and safety reasons. Of those gliptins currently marketed worldwide, linagliptin is, so far, the only drug that does not require dose adjustment in all stages of renal insufficiency.⁴⁵ Tenzeligliptin also does not require dose adjustment because the drug and its main metabolite are eliminated via hepatic routes; renal elimination accounts for up to 20%.⁴⁶

All DPP-4 inhibitors have relatively low target dissociation rates. However, only linagliptin exhibits a fast on-rate and an extraordinarily slow off-rate leading to a residence time of approximately 5.5 h. The compound has affinity in the single-digit picomolar range and is therefore orders of magnitude lower than DPP-4 protein concentrations in plasma and tissues. Consequently, the drug undergoes continuous rebinding events that lead to the observed phenomenon of target-mediated drug deposition in plasma and tissues, has a terminal pharmacokinetic half-life of approximately 100 h as determined from

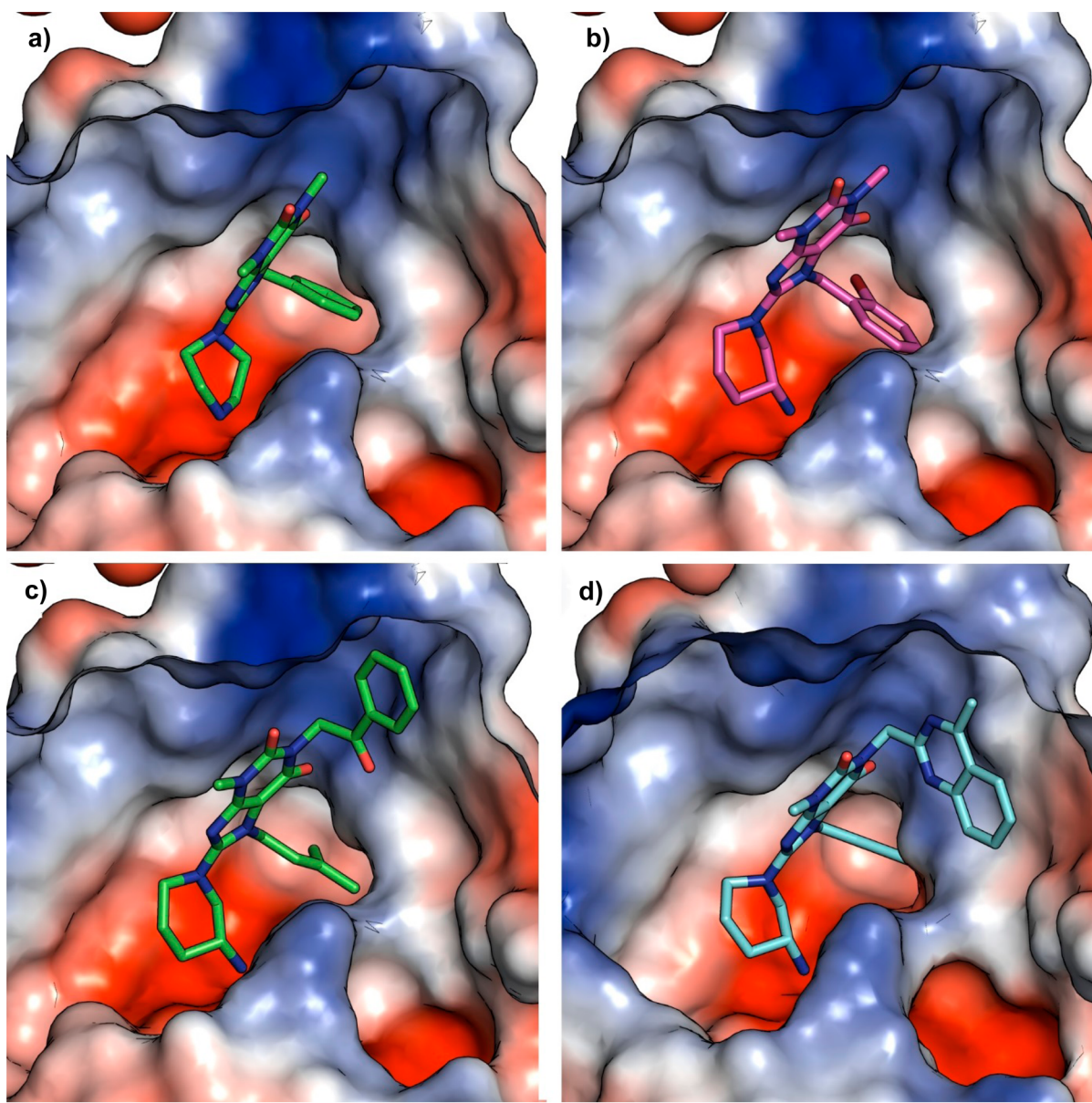


Figure 7. X-ray structures of linagliptin precursors in complex with DPP-4 in a surface representation with calculated surface charges (Pymol). (a) shows the initial HTS hit (2AJ8, compound 1). (b) is the X-ray structure of a Br-derivative of compound 2 (compound 4; PDB accession code 5LLS (Supporting Information Figure S6, Table S2)). (c) shows compound 3 modeled in the active site, and (d) is the X-ray structure of linagliptin (2RGU). PDB accession codes of X-ray structures are indicated in parentheses when applicable.

clinical data,⁴⁷ and has a high compound efficacy at very low therapeutic dose because of a high target occupancy at stoichiometric concentrations. The additional rapid elimination of free drug leads to low systemic exposure and a low rate of renal clearance.

CONCLUSIONS

In this study, DPP-4 inhibitors currently approved for the treatment of type 2 diabetes were investigated, namely, sitagliptin, vildagliptin, saxagliptin, linagliptin, alogliptin, and teneligliptin, as well as a congeneric series of linagliptin precursors. SPR and ITC methods were used to evaluate binding kinetics (k_{on} , k_{off} , K_{D}) and thermodynamics (ΔH , ΔS), and structural information on ligand–DPP-4 complexes was used to discuss and interpret the biophysical data in the context of three-dimensional structures.

The gliptins bind to DPP-4 in a rapid association regime (10^5 – 10^7 $\text{M}^{-1} \text{s}^{-1}$). This is because of a Coulomb attraction between the negatively charged Glu dyad within the DPP-4 active site and the positive charge on the ammonium moieties of the ligands. The fact that primary amines, which have a larger charge build-up, associate faster than secondary amines demonstrates that localized surface charges on both ligand and receptor contribute to binding velocity. The slow dissociation of some gliptins (10^{-4} – 10^{-5} s^{-1}) is a result of two types of kinetic barriers: the breaking of the covalent bond of the cyanopyrrolidines (saxagliptin and vildagliptin) with the associated enlarged activation barrier for dissociation, and the dissolution of strong polar and extensive hydrophobic interactions (linagliptin and teneligliptin). Finally, pairs of DPP-4 inhibitors with similar modes of binding and similar protein-induced conformational changes show dissimilar bind-

ing kinetics. Therefore, in this scenario and in contrast to other reports, conformational change has no dominant role in determining binding kinetics.

The series of congeneric linagliptin precursors also rapidly associate. The decrease in k_{off} during compound progression correlates with binding affinity. The improvements in off-rates were achieved through moieties that either form enhanced hydrogen bonding interactions or cover larger hydrophobic surface areas.

All DPP-4 inhibitors exhibit a dominant enthalpic contribution to the free energy of binding. This does not change during LO. The increase in binding affinity is fully reflected by increasing binding enthalpy. Finally, the significant increase in lipophilicity does not influence entropic effects but increases enthalpic contributions.

Using biophysical and biochemical methods, we have shown that linagliptin has, by far, the highest affinity for DPP-4 with a K_D of 0.0066 nM. This is approximately 45 times more potent than saxagliptin, the second best compound within the gliptin class. Further, the residence time is 4 times longer for linagliptin than for saxagliptin or vildagliptin. The extremely high affinity of linagliptin for DPP-4, the fast association rates, and the fact that DPP-4 target concentrations are much greater than the K_D strongly suggest that rebinding is the dominant mechanism behind the prolongation of the pharmacokinetic terminal half-life of linagliptin. Despite an increasing number of recent examples in the literature, the molecular determinants of binding kinetics remain poorly understood.^{12,21} With the biophysical data and their interpretation given in this manuscript, we intend to improve current understanding of the underlying phenomena.

■ EXPERIMENTAL SECTION

Materials. Teneeligliptin hydrobromide was purchased from BOC Sciences (Creative Dynamics Inc., NY, USA) and had a stated purity of >98%. All other DPP-4 inhibitors were synthesized in-house at Boehringer Ingelheim Pharma GmbH & Co. KG, Biberach, Germany, and had a general purity of >95% as determined by high performance liquid chromatography and proton nuclear magnetic resonance (¹H NMR). Recombinant human DPP-4 enzyme (aa 39-766) was purchased from Proteros Biostructures GmbH (Munich, Germany).

Inhibition of DPP-4 Activity from Human Blood or Recombinant Enzyme. Compounds were dissolved in DMSO (final concentration 0.1%), and inhibition of human recombinant DPP-4 was assayed in black 96-well plates in assay buffer (100 mM Tris, 100 mM NaCl, adjusted to pH 7.8 with HCl or NaOH) in the presence of 80 μ M substrate (H-Ala-Pro-7-amido-4-trifluoromethyl-coumarin [AlaPro-AFC]; from Bachem AG, Bubendorf, Switzerland) at room temperature for 1 h. The final volume was 100 μ L, and the final protein concentration was 10 ng/well corresponding to 1.2 nM. Fluorescence was detected using a Wallac Victor 1420 multilabel counter (PerkinElmer, Rodgau, Germany) at an excitation wavelength of 405 nm and an emission wavelength of 535 nm. Human plasma was obtained from healthy male and female individuals and collected in heparin-coated tubes (Sarstedt AG & Co, Nümbrecht, Germany); DPP-4 activity was assayed as described above.

Surface Plasmon Resonance Experiments. DPP-4 was immobilized onto a CM5 chip (GE Healthcare Bio-Sciences AB, Uppsala, Sweden) by amine coupling in 10 mM Na acetate at pH 5.5. Binding studies were performed using a Biacore T200 instrument (GE Healthcare) at 25 °C in 20 mM Tris, pH 7.3, 150 mM NaCl, 0.05% Tween 20, and 1% DMSO at a flow rate of 30 μ L/min.

The interaction analyses were performed in the single-cycle kinetic mode using 120 s association time and 7200 s dissociation time at the following DPP-4 inhibitor concentrations: linagliptin 0.24, 0.74, 2.2,

6.6, and 20 nM; vildagliptin and saxagliptin 0.8, 4, 20, 100, and 500 nM; teneeligliptin 0.16, 0.8, 4, 20, and 100 nM.

Alogliptin and sitagliptin were analyzed in the multicycle kinetic analysis mode using 120 s association time and 300 s (or 1800 s) dissociation time at analyte concentrations of 1.56, 3.1, 6.25, 12.5, 25, 50, and 100 nM. Kinetic parameters were analyzed using the Biacore T200 evaluation software 2.0 with the implemented 1:1 binding model.

Isothermal Titration Calorimetry Analysis. Experiments using isothermal titration calorimetry were conducted on a MicroCal iTC200 instrument with DPP-4 that had been passed through a PD-10 desalting column (GE Healthcare) equilibrated with 20 mM Tris, pH 7.3, and 150 mM NaCl. Complete saturation of 5 μ M DPP-4 inhibitor was typically achieved by injecting $18 \times 2 \mu$ L aliquots of 40 μ M DPP-4 at 25 °C. Values obtained by reverse titration experiments were in good agreement.

The thermodynamic binding parameters were extracted by nonlinear regression analysis of the binding isotherms (MicroCal Origin software, version 7.0). A single-site binding model was applied yielding the binding enthalpy (ΔH), stoichiometry (n), entropy (ΔS), and association constant (K_a).

To ensure that the observed binding enthalpy was not affected by net proton release or uptake upon ligand binding, control titrations in phosphate buffer were performed. The observed ΔH from the titration experiments were plotted against $\Delta H_{\text{ionization}}$ of the two buffers. The slope of the line (which gives the number of protons released by the buffers) does not indicate proton release or uptake.

It should be noted that because of the high affinity of tested ligands, the values for the association constant K_a may be prone to error. Therefore, a competition ITC experiment was conducted for linagliptin, the most potent compound studied, in the presence of compound 1. These data were used to validate the thermodynamic parameters derived from direct titration experiments (Supporting Information Figure S2).

■ ASSOCIATED CONTENT

Supporting Information

The Supporting Information is available free of charge on the ACS Publications website at DOI: 10.1021/acs.jmedchem.6b00475.

IC₅₀ values of approved DPP-4 inhibitors on human recombinant DPP-4 and plasma-derived DPP-4, kinetic on–off rate plot of different DPP-4 inhibitors, isothermal titration of linagliptin in the presence of a competition ligand, isothermal titration calorimetry of DPP-4 inhibitors, isothermal titration calorimetry of linagliptin precursors, measured pK_a and lipophilicity data (log *D*) for tested compounds, crystal structure of compound 4 in porcine DPP-4, crystallographic data collection and refinement statistics (PDF)

Molecular formula strings and some data (CSV)

■ AUTHOR INFORMATION

Corresponding Author

*E-mail: herbert.nar@boehringer-ingelheim.com. Phone: +49 (0)7351 54 2888. Fax: +49 (0)7351 54 2165.

Author Contributions

G.S. conceived the experimental design, analyzed the data, and wrote the manuscript. T.K. contributed to research design and helped to prepare the manuscript. Y.H. carried out experiments. R.A.B. contributed to research design. H.N. contributed to research design, analyzed the data, and wrote the manuscript.

Notes

The authors declare the following competing financial interest(s): All authors are employees of Boehringer Ingelheim.

■ ACKNOWLEDGMENTS

This work was supported by Boehringer Ingelheim. The authors were fully responsible for all content and editorial decisions, were involved at all stages of manuscript development, and have approved the final version. We thank Dr. Silke Retlich and Dr. Holger Fuchs for helpful discussions regarding the pharmacokinetic aspects in the manuscript, Dr. Matthias Eckhardt for synthesis of linagliptin and the precursors, and Dr. Michael Blaesse, Proteros Biostructures, for determining the initial costructure of compound **4** with porcine DPP-4. Editorial assistance, supported by Boehringer Ingelheim, was provided by Paul MacCallum, Ph.D., of Envision Scientific Solutions during the preparation of this manuscript.

■ ABBREVIATIONS USED

DPP-4, dipeptidyl peptidase-4; GIP, glucose-dependent insulinotropic peptide; GLP-1, glucagon-like peptide-1; IC₅₀, half maximal inhibitory concentration; ITC, isothermal titration calorimetry; LO, lead optimization; SPR, surface plasmon resonance; τ , residence time, reciprocal of k_{off}

■ REFERENCES

- (1) Kieffer, T. J.; McIntosh, C. H.; Pederson, R. A. Degradation of glucose-dependent insulinotropic polypeptide and truncated glucagon-like peptide 1 in vitro and in vivo by dipeptidyl peptidase IV. *Endocrinology* **1995**, *136*, 3585–3596.
- (2) Meier, J. J.; Nauck, M. A.; Schmidt, W. E.; Gallwitz, B. Gastric inhibitory polypeptide: the neglected incretin revisited. *Regul. Pept.* **2002**, *107*, 1–13.
- (3) Egan, J. M.; Bulotta, A.; Hui, H.; Perfetti, R. GLP-1 receptor agonists are growth and differentiation factors for pancreatic islet beta cells. *Diabetes/Metab. Res. Rev.* **2003**, *19*, 115–123.
- (4) Murphy, K. G.; Dhillon, W. S.; Bloom, S. R. Gut peptides in the regulation of food intake and energy homeostasis. *Endocr. Rev.* **2006**, *27*, 719–727.
- (5) McIntosh, C. H. Dipeptidyl peptidase IV inhibitors and diabetes therapy. *Front. Biosci., Landmark Ed.* **2008**, *13*, 1753–1773.
- (6) Rasmussen, H. B.; Branner, S.; Wiberg, F. C.; Wagtmann, N. Crystal structure of human dipeptidyl peptidase IV/CD26 in complex with a substrate analog. *Nat. Struct. Biol.* **2003**, *10*, 19–25.
- (7) Golightly, L. K.; Drayna, C. C.; McDermott, M. T. Comparative clinical pharmacokinetics of dipeptidyl peptidase-4 inhibitors. *Clin. Pharmacokinet.* **2012**, *51*, 501–514.
- (8) Liu, Y.; Hu, Y.; Liu, T. Recent advances in non-peptidomimetic dipeptidyl peptidase 4 inhibitors: medicinal chemistry and preclinical aspects. *Curr. Med. Chem.* **2012**, *19*, 3982–3999.
- (9) Nabeno, M.; Akahoshi, F.; Kishida, H.; Miyaguchi, I.; Tanaka, Y.; Ishii, S.; Kadowaki, T. A comparative study of the binding modes of recently launched dipeptidyl peptidase IV inhibitors in the active site. *Biochem. Biophys. Res. Commun.* **2013**, *434*, 191–196.
- (10) Yoshida, T.; Akahoshi, F.; Sakashita, H.; Kitajima, H.; Nakamura, M.; Sonda, S.; Takeuchi, M.; Tanaka, Y.; Ueda, N.; Sekiguchi, S.; Ishige, T.; Shima, K.; Nabeno, M.; Abe, Y.; Anabuki, J.; Soejima, A.; Yoshida, K.; Takashina, Y.; Ishii, S.; Kiuchi, S.; Fukuda, S.; Tsutsumiuchi, R.; Kosaka, K.; Murozono, T.; Nakamaru, Y.; Utsumi, H.; Masutomi, N.; Kishida, H.; Miyaguchi, I.; Hayashi, Y. Discovery and preclinical profile of teneligliptin (3-[(2S,4S)-4-[4-(3-methyl-1-phenyl-1H-pyrazol-5-yl)piperazin-1-yl]pyrrolidin-2-yl carbonyl]-thiazolidine): a highly potent, selective, long-lasting and orally active dipeptidyl peptidase IV inhibitor for the treatment of type 2 diabetes. *Bioorg. Med. Chem.* **2012**, *20*, 5705–5719.
- (11) Eckhardt, M.; Langkopf, E.; Mark, M.; Tadayyon, M.; Thomas, L.; Nar, H.; Pfengle, W.; Guth, B.; Lotz, R.; Sieger, P.; Fuchs, H.; Himmelsbach, F. 8-(3-(R)-aminopiperidin-1-yl)-7-but-2-ynyl-3-methyl-1-(4-methyl-quinazolin-2-ylmethyl)-3,7-dihydropurine-2,6-dione (BI 1356), a highly potent, selective, long-acting, and orally bioavailable DPP-4 inhibitor for the treatment of type 2 diabetes. *J. Med. Chem.* **2007**, *50*, 6450–6453.
- (12) Cusack, K. P.; Wang, Y.; Hoemann, M. Z.; Marjanovic, J.; Heym, R. G.; Vasudevan, A. Design strategies to address kinetics of drug binding and residence time. *Bioorg. Med. Chem. Lett.* **2015**, *25*, 2019–2027.
- (13) Andersson, K.; Karlsson, R.; Lofas, S.; Franklin, G.; Hamalainen, M. D. Label-free kinetic binding data as a decisive element in drug discovery. *Expert Opin. Drug Discovery* **2006**, *1*, 439–446.
- (14) Freire, E. Do enthalpy and entropy distinguish first in class from best in class? *Drug Discovery Today* **2008**, *13*, 869–874.
- (15) Ladbury, J. E.; Klebe, G.; Freire, E. Adding calorimetric data to decision making in lead discovery: a hot tip. *Nat. Rev. Drug Discovery* **2010**, *9*, 23–27.
- (16) Nunez, S.; Venhorst, J.; Kruse, C. G. Target-drug interactions: first principles and their application to drug discovery. *Drug Discovery Today* **2012**, *17*, 10–22.
- (17) Klebe, G. Applying thermodynamic profiling in lead finding and optimization. *Nat. Rev. Drug Discovery* **2015**, *14*, 95–110.
- (18) Liu, Y.; Hu, Y. Novel DPP-4 inhibitors against diabetes. *Future Med. Chem.* **2014**, *6*, 793–808.
- (19) Tummino, P. J.; Copeland, R. A. Residence time of receptor-ligand complexes and its effect on biological function. *Biochemistry* **2008**, *47*, 5481–5492.
- (20) Thomas, L.; Eckhardt, M.; Langkopf, E.; Tadayyon, M.; Himmelsbach, F.; Mark, M. (R)-8-(3-amino-piperidin-1-yl)-7-but-2-ynyl-3-methyl-1-(4-methyl-quinazolin-2-ylmethyl)-3,7-dihydropurine-2,6-dione (BI 1356), a novel xanthine-based dipeptidyl peptidase 4 inhibitor, has a superior potency and longer duration of action compared with other dipeptidyl peptidase-4 inhibitors. *J. Pharmacol. Exp. Ther.* **2008**, *325*, 175–182.
- (21) Pan, A. C.; Borhani, D. W.; Dror, R. O.; Shaw, D. E. Molecular determinants of drug-receptor binding kinetics. *Drug Discovery Today* **2013**, *18*, 667–673.
- (22) Wang, A.; Dorso, C.; Kopcho, L.; Locke, G.; Langish, R.; Harstad, E.; Shipkova, P.; Marcinkeviciene, J.; Hamann, L.; Kirby, M. S. Potency, selectivity and prolonged binding of saxagliptin to DPP4: maintenance of DPP4 inhibition by saxagliptin in vitro and ex vivo when compared to a rapidly-dissociating DPP4 inhibitor. *BMC Pharmacol.* **2012**, *12*, 2.
- (23) Metzler, W. J.; Yanchunas, J.; Weigelt, C.; Kish, K.; Klei, H. E.; Xie, D.; Zhang, Y.; Corbett, M.; Tamura, J. K.; He, B.; Hamann, L. G.; Kirby, M. S.; Marcinkeviciene, J. Involvement of DPP-IV catalytic residues in enzyme-saxagliptin complex formation. *Protein Sci.* **2008**, *17*, 240–250.
- (24) Schmidtke, P.; Luque, F. J.; Murray, J. B.; Barril, X. Shielded hydrogen bonds as structural determinants of binding kinetics: application in drug design. *J. Am. Chem. Soc.* **2011**, *133*, 18903–18910.
- (25) Copeland, R. A. Conformational adaptation in drug-target interactions and residence time. *Future Med. Chem.* **2011**, *3*, 1491–1501.
- (26) Biela, A.; Nasief, N. N.; Betz, M.; Heine, A.; Hangauer, D.; Klebe, G. Dissecting the hydrophobic effect on the molecular level: the role of water, enthalpy, and entropy in ligand binding to thermolysin. *Angew. Chem., Int. Ed.* **2013**, *52*, 1822–1828.
- (27) Steuber, H.; Heine, A.; Klebe, G. Structural and thermodynamic study on aldose reductase: nitro-substituted inhibitors with strong enthalpic binding contribution. *J. Mol. Biol.* **2007**, *368*, 618–638.
- (28) Abel, R.; Young, T.; Farid, R.; Berne, B. J.; Friesner, R. A. Role of the active-site solvent in the thermodynamics of factor Xa ligand binding. *J. Am. Chem. Soc.* **2008**, *130*, 2817–2831.
- (29) Young, T.; Abel, R.; Kim, B.; Berne, B. J.; Friesner, R. A. Motifs for molecular recognition exploiting hydrophobic enclosure in protein-ligand binding. *Proc. Natl. Acad. Sci. U. S. A.* **2007**, *104*, 808–813.
- (30) Nguyen, C. N.; Cruz, A.; Gilson, M. K.; Kurtzman, T. Thermodynamics of Water in an Enzyme Active Site: Grid-Based Hydration Analysis of Coagulation Factor Xa. *J. Chem. Theory Comput.* **2014**, *10*, 2769–2780.

- (31) Nguyen, C. N.; Young, T. K.; Gilson, M. K. Grid inhomogeneous solvation theory: hydration structure and thermodynamics of the miniature receptor cucurbit[7]uril. *J. Chem. Phys.* **2012**, *137*, 044101.
- (32) Ruhmann, E.; Betz, M.; Fricke, M.; Heine, A.; Schafer, M.; Klebe, G. Thermodynamic signatures of fragment binding: Validation of direct versus displacement ITC titrations. *Biochim. Biophys. Acta, Gen. Subj.* **2015**, *1850*, 647–656.
- (33) Schuck, P.; Zhao, H. The role of mass transport limitation and surface heterogeneity in the biophysical characterization of macromolecular binding processes by SPR biosensing. *Methods Mol. Biol.* **2010**, *627*, 15–54.
- (34) Copeland, R. A.; Pompliano, D. L.; Meek, T. D. Drug-target residence time and its implications for lead optimization. *Nat. Rev. Drug Discovery* **2006**, *5*, 730–739.
- (35) Ferenczy, G. G.; Keseru, G. M. Thermodynamics guided lead discovery and optimization. *Drug Discovery Today* **2010**, *15*, 919–932.
- (36) Holdgate, G. A. Thermodynamics of binding interactions in the rational drug design process. *Expert Opin. Drug Discovery* **2007**, *2*, 1103–1114.
- (37) Swinney, D. C. The role of binding kinetics in therapeutically useful drug action. *Curr. Opin. Drug Discovery Dev.* **2009**, *12*, 31–39.
- (38) Englert, L.; Biela, A.; Zayed, M.; Heine, A.; Hangauer, D.; Klebe, G. Displacement of disordered water molecules from hydrophobic pocket creates enthalpic signature: binding of phosphoramidate to the S(1)'-pocket of thermolysin. *Biochim. Biophys. Acta, Gen. Subj.* **2010**, *1800*, 1192–1202.
- (39) Krimmer, S. G.; Betz, M.; Heine, A.; Klebe, G. Methyl, ethyl, propyl, butyl: futile but not for water, as the correlation of structure and thermodynamic signature shows in a congeneric series of thermolysin inhibitors. *ChemMedChem* **2014**, *9*, 833–846.
- (40) Scheen, A. J. A review of gliptins in 2011. *Expert Opin. Pharmacother.* **2012**, *13*, 81–99.
- (41) Scheen, A. J. A review of gliptins for 2014. *Expert Opin. Pharmacother.* **2015**, *16*, 43–62.
- (42) Graefe-Mody, U.; Retlich, S.; Friedrich, C. Clinical pharmacokinetics and pharmacodynamics of linagliptin. *Clin. Pharmacokinet.* **2012**, *51*, 411–427.
- (43) Fuchs, H.; Tillement, J. P.; Urien, S.; Greischel, A.; Roth, W. Concentration-dependent plasma protein binding of the novel dipeptidyl peptidase 4 inhibitor BI 1356 due to saturable binding to its target in plasma of mice, rats and humans. *J. Pharm. Pharmacol.* **2009**, *61*, 55–62.
- (44) Retlich, S.; Withopf, B.; Greischel, A.; Staab, A.; Jaehde, U.; Fuchs, H. Binding to dipeptidyl peptidase-4 determines the disposition of linagliptin (BI 1356)—investigations in DPP-4 deficient and wildtype rats. *Biopharm. Drug Dispos.* **2009**, *30*, 422–436.
- (45) Graefe-Mody, U.; Friedrich, C.; Port, A.; Ring, A.; Retlich, S.; Heise, T.; Halabi, A.; Woerle, H. J. Effect of renal impairment on the pharmacokinetics of the dipeptidyl peptidase-4 inhibitor linagliptin(*). *Diabetes, Obes. Metab.* **2011**, *13*, 939–946.
- (46) Halabi, A.; Maatouk, H.; Siegler, K. E.; Faisst, N.; Lufft, V.; Klaue, N. Pharmacokinetics of teneligliptin in subjects with renal impairment. *Clin. Pharmacol. Drug Dev.* **2013**, *2*, 246–254.
- (47) Retlich, S.; Duval, V.; Graefe-Mody, U.; Jaehde, U.; Staab, A. Impact of target-mediated drug disposition on Linagliptin pharmacokinetics and DPP-4 inhibition in type 2 diabetic patients. *J. Clin. Pharmacol.* **2010**, *50*, 873–885.
- (48) Kim, D.; Wang, L.; Beconi, M.; Eiermann, G. J.; Fisher, M. H.; He, H.; Hickey, G. J.; Kowalchick, J. E.; Leiting, B.; Lyons, K.; Marsilio, F.; McCann, M. E.; Patel, R. A.; Petrov, A.; Scapin, G.; Patel, S. B.; Roy, R. S.; Wu, J. K.; Wyvratt, M. J.; Zhang, B. B.; Zhu, L.; Thornberry, N. A.; Weber, A. E. (2R)-4-oxo-4-[3-(trifluoromethyl)-5,6-dihydro[1,2,4]triazolo[4,3-a]pyrazin-7(8H)-yl]-1-(2,4,5-trifluorophenyl)butan-2-amine: a potent, orally active dipeptidyl peptidase IV inhibitor for the treatment of type 2 diabetes. *J. Med. Chem.* **2005**, *48*, 141–151.
- (49) Zhang, Z.; Wallace, M. B.; Feng, J.; Stafford, J. A.; Skene, R. J.; Shi, L.; Lee, B.; Aertgeerts, K.; Jennings, A.; Xu, R.; Kassel, D. B.; Kaldor, S. W.; Navre, M.; Webb, D. R.; Gwaltney, S. L. Design and synthesis of pyrimidinone and pyrimidinedione inhibitors of dipeptidyl peptidase IV. *J. Med. Chem.* **2011**, *54*, 510–524.